International Journal of Engineering, Mathematical and Physical Sciences
ISSN: 2517-9934
Vol:11, No:2, 2017

Effects of Thermal Radiation on Mixed Convection in a MHD Nanofluid Flow over a Stretching Sheet Using a Spectral Relaxation Method

Nageeb A. H. Haroun, Sabyasachi Mondal, Precious Sibanda

***Abstract*—**The effects of thermal radiation, Soret and Dufour parameters on mixed convection and nanofluid flow over a stretching sheet in the presence of a magnetic field are investigated. The flow is subject to temperature dependent viscosity and a chemical reaction parameter. It is assumed that the nanoparticle volume fraction at the wall may be actively controlled. The physical problem is modelled using systems of nonlinear differential equations which have been solved numerically using a spectral relaxation method. In addition to the discussion on heat and mass transfer processes, the velocity, nanoparticles volume fraction profiles as well as the skin friction coefficient are determined for different important physical parameters. A comparison of current findings with previously published results for some special cases of the problem shows an excellent agreement.

***Keywords*—**Non-isothermal wedge, thermal radiation, nanofluid, magnetic field, Soret and Dufour effects.

I. Introduction

MAGNETOHYDRODYNAMICS (MHD) flow and heat and mass transfer over a stretching surface has applications in polymer technology, glass-fiber production and in metallurgical industries. Many metallurgical processes involve cooling continuous strips or filaments by drawing them through a quiescent fluid. The properties of the final product depend on the rate of cooling which can be controlled by drawing such strips in an electrically conducting fluid subject to a magnetic field to achieve the desired characteristics of the final product. Indeed, many engineering processes, such as transport via conveyor belts, possess the characteristics of a moving continuous surface (see Subhas and Veena [1], Prasad et al. [2]). Blasius [3] was the first to report the boundary layer flow over a flat plate in a uniform free stream. Howarth [4] provided numerical solutions to the Blasius problem while Crane [5] expanded the study to stretched surfaces. Other features such as porosity, magnetic field effects and viscoelasticity or permeable surfaces, were studied by, among others, Gupta and Gupta [6]. Some recent contributions have come from Aiyesimi et al. [7]. Liao [8] and Xu et al. [9] obtained series solutions of the boundary layer equations.

In the past few years, convective heat and mass transfer in nanofluids has become a topic of major contemporary interest. Nanofluids have a significant role in enhancing the heat transfer properties of fluids, for instance, nanofluids have been shown to have higher thermal conductivity rates compared to common fluids such as water which makes these fluids ideal as advanced heat transfer fluids. Masuda et al . [10] for instance have suggested the use of nanofluids in cooling advanced nuclear systems. The most important properties of nanofluids are enhanced effective fluid thermal conductivity and heat transfer coefficient (see [11]-[17]). Studies on steady and unsteady nanofluid flow due to a stretching sheet were reported by Gbadeyan et al. [18], Subhakar and Gangadhar [19], Mahapatra et al. [20], Shakhaoath et al. [21] and Singh et al. [22]. Rohni et al. [23] presented a numerical solution for the unsteady flow over a continuously shrinking surface with wall mass suction using the nanofluid model proposed by Buongiorno [24]. In addition, a numerical study of natural convection in partially heated rectangular enclosures filled with nanofluids was carried out by Oztop and Abu-Nada [25]. Gharagozloo et al. [26] investigated aggregation and thermal conductivity in nanofluids while Philip et al. [27] proposed a nanofluid with tunable thermal properties. Recently, Haroun et al. [28] studied unsteady MHD mixed convection in a nanofluid due to a stretching/shrinking surface with suction/injection using the spectral relaxation method.

The aim of the present study is to analyze thermal radiation, Soret and Dufour effects on steady mixed convection in boundary layer flow of a nanofluid over a non-isothermal with a chemical reaction and viscous dissipation using spectral relaxation method (SRM) (see Motsa [29]). A comparative study for a special case is presented which shows excellent agreement with Yih [30].

II. Mathematical Formulations

Consider steady two-dimensional incompressible nanofluid flow over a non-isothermal stretching wedge (see Fig. 1). The temperature and nanoparticle concentration at the stretching surface are T_w and C_w respectively, and in the ambient nanofluid these are T_∞ and C_∞, respectively. The radiation heat flux in the x-direction is negligible compared to the flux in the y-direction. The x and y directions are in the plane of, and perpendicular to the sheet, respectively. The continuity, momentum, heat and mass transfer equations of a steady, an incompressible nanofluid boundary layer flow are (see Tiwari and Das [31])

N. A. H. Haroun and P. Sibanda are with the School of Mathematics, Statistics and Computer Science, University of KwaZulu-Natal, Private Bag X01 Scottsville 3209, Pietermaritzburg, South Africa.

S. Mondal is with the School of Mathematics, Statistics and Computer Science, University of KwaZulu-Natal, Private Bag X01 Scottsville 3209, Pietermaritzburg, South Africa (corresponding author, e-mail: sabya.mondal.2007@gmail.com).

$$\frac{\partial u}{\partial x}+\frac{\partial v}{\partial y}=0, \tag{1}$$

$$u\frac{\partial u}{\partial x}+v\frac{\partial u}{\partial y}=\nu_{nf}\frac{\partial^2 u}{\partial y^2}-\frac{1}{\rho_{nf}}\frac{\partial p}{\partial x}-u\left\{\frac{\sigma B_0^2}{\rho_{nf}}\right\} +g\beta_T(T-T\infty)+g\beta_C(C-C\infty), \tag{2}$$

$$u\frac{\partial T}{\partial x}+v\frac{\partial T}{\partial y}=\alpha_{nf}\frac{\partial^2 T}{\partial y^2}-\frac{1}{(\rho cp)_{nf}}\frac{\partial q_r}{\partial y} +\frac{\rho_f D_m K_T}{C_s(\rho cp)_{nf}}\frac{\partial^2 C}{\partial^2 y}+\frac{\nu_{nf}}{(cp)_{nf}}\left(\frac{\partial u}{\partial y}\right)^2, \tag{3}$$

$$u\frac{\partial C}{\partial x}+v\frac{\partial C}{\partial y}=D_m\frac{\partial^2 C}{\partial y^2}+\frac{D_m K_T}{T_m}\frac{\partial^2 T}{\partial y^2}-R(C-C_\infty), \tag{4}$$

where u and v are the fluid velocity components in the x and y directions, respectively, ν_{nf}, p, ρ_{nf}, σ, B_0, μ_{nf}, g are the nanofluid kinematic viscosity, the pressure, nanofluid density, electrical conductivity, the uniform magnetic field in the y-direction, the effective dynamic viscosity of the nanofluid and gravitational acceleration. β_T, β_C, T, C, α_{nf}, $(\rho cp)_{nf}$ are the volumetric thermal expansion coefficient, volumetric solutal expansion coefficient, temperature of fluid in the boundary layer, fluid solutal concentration, the thermal diffusivity of the nanofluid, the nanofluid heat capacitance respectively. ρ_f, D_m, K_T, C_s, $(cp)_{nf}$, T_m, R are the density of the base fluid, the mass diffusivity of the concentration, thermal diffusion ratio, concentration susceptibility, specific heat of fluid at constant pressure, mean fluid temperature and the chemical reaction parameter respectively. Here q_r is the radiation heat flux given by

$$q_r=-\frac{4\sigma^*}{3K^*}\frac{\partial T^4}{\partial y} \tag{5}$$

where σ^* is the Stefen-Boltzmann constant and K^* is the Rosseland mean absorption coefficient. Expanding T^4 about T_∞ we obtain, $T^4\cong 4T_\infty^3T-3T_\infty^4$, (see Singh et al. [22]).
For a uniform- stream, the momentum equation (2) becomes

$$U_\infty\frac{dU_\infty}{dx}=-\frac{1}{\rho_{nf}}\frac{\partial p}{\partial x}-\frac{\sigma B_0^2}{\rho_{nf}}U_\infty \tag{6}$$

where $U_\infty=ax^n$ is the velocity of the potential flow, $n=\beta/(2-\beta)$, and β is the Hartree pressure gradient parameter with $\beta=\Omega/\pi$ for a total angle of the wedge, a is a positive real number.
Substituting (6) in (2) and (5) in (3), the transport equations are written as

$$u\frac{\partial u}{\partial x}+v\frac{\partial u}{\partial y}=\nu_{nf}\frac{\partial^2 u}{\partial y^2}+U_\infty\frac{dU_\infty}{dx}+(U_\infty-u)\left\{\frac{\sigma B_0^2}{\rho_{nf}}\right\} +g\beta_T(T-T\infty)+g\beta_C(C-C\infty), \tag{7}$$

$$u\frac{\partial T}{\partial x}+v\frac{\partial T}{\partial y}=\alpha_{nf}\frac{\partial^2 T}{\partial y^2}+\frac{1}{(\rho cp)_{nf}}\frac{16\sigma^* T_\infty^3}{3K^*}\frac{\partial^2 T}{\partial^2 y} +\frac{\rho_f D_m K_T}{C_s(\rho cp)_{nf}}\frac{\partial^2 C}{\partial^2 y}+\frac{\nu_{nf}}{(cp)_{nf}}\left(\frac{\partial u}{\partial y}\right)^2, \tag{8}$$

subject to the boundary conditions

$$\begin{aligned} &u=\ v=0,\ T=T_{\rm w}(x)=T_\infty+T_0x^{2n},\\ &C=C_{\rm w}(x)=C_\infty+C_0x^{2n} \quad \text{at} \quad y=0,\\ &u\to U_\infty=ax^n,\ T=T_\infty,\ C=C_\infty\\ &\quad \text{as} \quad y\to\infty,\ 0\le n\le 1, \end{aligned} \tag{9}$$

and initial conditions

$$u=0,\quad v=0,\quad T=T_{\rm w},\ C=C_{\rm w},\qquad \forall\ x,y, \tag{10}$$

where T_0 and C_0, are positive real numbers. When $n=0$, we have the boundary - layer flow over a stationary flat plate. When $n=1$, we obtain flow near the stagnation point of an infinite wall.

The effective viscosity of the nanofluid is (see Brinkman [32])

$$\mu_{nf}=\frac{\mu_f}{(1-\phi)^{2.5}}, \tag{11}$$

where ϕ and μ_f are the solid volume fraction of nanoparticles and the dynamic viscosity of the base fluid. In (1)-(4);

$$\begin{aligned} &(\rho c_p)_{nf}=(1-\phi)(\rho c_p)_f+\phi(\rho c_p)_s\\ &\rho_{nf}=(1-\phi)\rho_f+\phi\rho_s,\\ &\nu_{nf}=\frac{\mu_{nf}}{\rho_{nf}},\alpha_{nf}=\frac{k_{nf}}{(\rho c_p)_{nf}},\\ &\frac{k_{nf}}{k_f}=\frac{(k_s+k_f)-2\phi(k_f-k_s)}{(k_s+k_f)+\phi(k_f-k_s)} \end{aligned} \tag{12}$$

where k_{nf}, k_f, k_s, ρ_s, $(\rho c_p)_f$, $(\rho c_p)_s$ are the thermal conductivity of the nanofluid, the thermal conductivity of the fluid, the thermal conductivity of the solid fractions, the density of the solid fractions, the heat capacity of base fluid and the effective heat capacity of nanoparticles, respectively, (see Abu-Nada [33]). $\alpha_f=k_f/(\rho c_p)_f$ and $\nu_f=\mu_f/\rho_f$ are the thermal diffusivity and kinetic viscosity of the base fluid, respectively.

The continuity equation (1) is satisfied by introducing a stream function $\psi(x,y)$ such that

$$u=\frac{\partial\psi}{\partial y},\quad v=-\frac{\partial\psi}{\partial x}. \tag{13}$$

Introducing the following non-dimensional variables, (see Yih [30])

$$\eta=\sqrt{\frac{U_\infty x}{\nu_f\xi}}\frac{y}{x},\xi=\frac{\sigma B_0^2}{\rho_{nf}U_\infty}x,\psi=\sqrt{U_\infty\nu_f x}f(\xi,\eta),$$

$$\theta(\xi,\eta)=\frac{T-T_\infty}{T_{\rm w}-T_\infty},\Phi(\xi,\eta)=\frac{C-C_\infty}{C_{\rm w}-C_\infty}. \tag{14}$$

where η and ξ are dimensionless variables. By using (14) the governing equations (4), (7) and (8) along with the boundary

conditions (9) are reduced to the following boundary value problem

$$f''' + \phi_1[\frac{n+1}{2} f f'' + n\left(1 - f'^2\right) + \xi(1 - f') + Gr_t\theta + Gr_c\phi] = \phi_1(1-n)\xi\left[f'\frac{\partial f'}{\partial \xi} - f''\frac{\partial f}{\partial \xi}\right], \quad (15)$$

$$\left(\frac{k_{nf}}{k_f}\frac{1}{Pr} + Nr\right)\theta'' + \phi_2\left[\frac{n+1}{2} f\theta' - 2nf'\theta\right] + D_f\Phi'' + \frac{Ec}{(1-\phi)^{2.5}}(f'')^2 = \phi_2(1-n)\xi\left[f'\frac{\partial \theta}{\partial \xi} - \theta'\frac{\partial f}{\partial \xi}\right], \quad (16)$$

$$\Phi'' + Sc\left[\frac{n+1}{2} f\Phi' - 2nf'\Phi - \gamma\Phi + Sr\theta''\right] = Sc(1-n)\xi\left[f'\frac{\partial \Phi}{\partial \xi} - \Phi'\frac{\partial f}{\partial \xi}\right], \quad (17)$$

subject to the boundary conditions

$$\begin{aligned} &f(\xi,0) = f'(\xi,0) = 0, \theta(\xi,0) = 1, \Phi(\xi,0) = 1, \\ &\text{when} \quad \eta = 0, \xi \geq 0, \\ &f'(\xi,\infty) = 1, \theta(\xi,\infty) = 0, \Phi(\xi,\infty) = 0, \\ &\text{when} \quad \eta \to \infty, \xi \geq 0, \end{aligned} \quad (18)$$

where primes denote differentiation with respect to η. The non-dimensional parameters appearing in (15)-(17) namely, Gr_t, Gr_c, Pr, Nr, Ec, Sc, D_f, γ and Sr denote the local temperature Grashof number, local concentration Grashof number, Prandtl number, thermal radiation parameter, Eckert number, the Schmidt number, Dufour number, scaled chemical reaction parameter and the Soret number.

The Eckert number represents the kinetic energy of the flow relative to the boundary layer enthalpy difference. The Dufour effect describes the energy flux created when a system is under a concentration gradient. These parameters are defined mathematically as

$$Gr_t = \frac{g\beta_T(T_w - T_\infty)x}{U_\infty^2}, Gr_c = \frac{g\beta_C(C_w - C_\infty)x}{U_\infty^2},$$
$$Pr = \frac{\nu_f}{\alpha_f}, Nr = \frac{16\sigma^* T_\infty^3}{3K^*(\rho cp)_f\nu_f}, Ec = \frac{U_\infty^2}{(cp)_f(T_w - T_\infty)},$$
$$Sc = \frac{\nu_f}{D_m}, D_f = \frac{D_m K_T(C_w - C_\infty)}{C_s C_p \nu_f (T_w - T_\infty)},$$
$$\nu_f = \frac{\mu_f}{\rho_f}, \gamma = \frac{Rx}{U_\infty}, Sr = \frac{D_m K_T(T_w - T_\infty)}{\nu_f T_m(C_w - C_\infty)}. \quad (19)$$

The nanoparticle volume fraction ϕ_1 and ϕ_2 are defined as

$$\phi_1 = (1-\phi)^{2.5}\left[1 - \phi + \phi\left(\frac{\rho_s}{\rho_f}\right)\right],$$
$$\phi_2 = \left[1 - \phi + \phi\frac{(\rho c)_s}{(\rho c)_f}\right]. \quad (20)$$

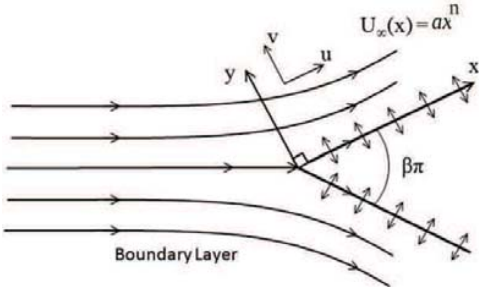

Fig. 1 Physical model and coordinate system

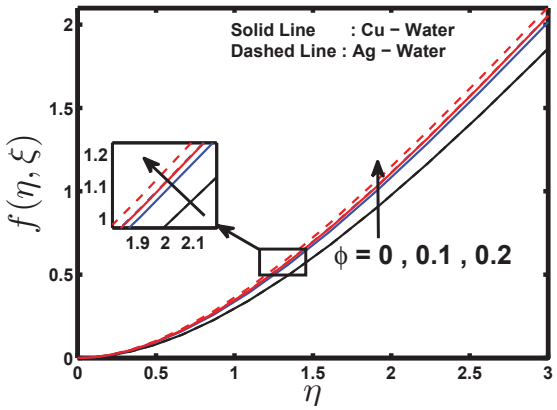

Fig. 2 Effect of change in the nanoparticle volume fraction values ϕ on velocity profiles for $Gr_t = 0.01$, $n = 0$, $Gr_c = 0.01$, $Nr = 10$, $Pr = 7$,$Ec = 10$, $D_f = 0.01$, $\gamma = 3$, $Sc = 1$, $Sr = 1$ and $\xi = 0.5$

III. Skin Friction, Heat and Mass Transfer Coefficients

Parameters of primary interest include the skin friction coefficient C_f, the local Nusselt number Nu_x, and the local Sherwood number Sh_x.

The shear stress at the surface of the wall τ_w is given by

$$\tau_w = -\mu_{nf}\left(\frac{\partial u}{\partial y}\right)_{y=0}$$
$$= -\frac{\mu_f}{(1-\phi)^{2.5}}\frac{U_\infty}{x}\sqrt{\frac{U_\infty x}{\nu_f}} f''(0,\xi). \quad (21)$$

The skin friction coefficient is defined as

$$C_f = \frac{2\tau_w}{\rho_f U_\infty^2}, \quad (22)$$

and using (21) in (22) we obtain

$$\frac{1}{2}(1-\phi)^{2.5}\sqrt{Re_x}\ \ C_f = -f''(0,\xi), \quad (23)$$

where Re_x is local Reynolds number given by

$$Re_x = \frac{U_\infty x}{\nu_f}. \quad (24)$$

The heat transfer rate at the surface is given by

$$q_w = -k_{nf}\left(\frac{\partial T}{\partial y}\right)_{y=0}$$

$$= -k_{nf}\frac{(T_w - T_\infty)}{x}\sqrt{\frac{U_\infty x}{\nu_f}}\ \theta'(0,\xi). \tag{25}$$

The Nusselt number is defined as

$$Nu_x = \frac{xq_w}{k_f\,(T_w - T_\infty)}. \tag{26}$$

Using (25) in (26), the wall heat transfer rate is obtained as

$$\frac{Nu_x}{\sqrt{Re_x}}\left(\frac{k_f}{k_{nf}}\right) = -\theta'(0,\xi). \tag{27}$$

The mass flux at the wall surface is given by

$$q_m = -D\left(\frac{\partial C}{\partial y}\right)_{y=0}$$

$$= -D\frac{(C_w - C_\infty)}{x}\sqrt{\frac{U_\infty x}{\nu_f}}\ \Phi'(0,\xi), \tag{28}$$

and the Sherwood number is defined as

$$Sh_x = \frac{xq_m}{D\,(C_w - C_\infty)}. \tag{29}$$

Using (2.28) in (2.29) the wall mass transfer rate is obtained as

$$\frac{Sh_x}{\sqrt{Re_x}} = -\Phi'(0,\xi). \tag{30}$$

IV. Some Particular Cases of Interest

In some limiting cases, (15)-(17) reduce to ordinary differential equations.

Case(1): For steady-state flow when $\phi = 0$ (regular fluid) with $\xi = 0$, $Gr_t = 0$ and $Gr_c = 0$, (15) is approximately as Yih [30]

$$f''' + \frac{n+1}{2}ff'' + n(1 - f'^2) = 0. \tag{31}$$

The solution of (31) is presented in Table (II) for the skin friction for various values of n.

Case(2) For a regular fluid when $\xi = 0$, and n, Nr, Ec, D_f, Gr_t and Gr_c are set to zero, (15) and (16) reduce to

$$f''' + \frac{1}{2}ff'' = 0. \tag{32}$$

$$\frac{1}{Pr}\theta'' + \frac{1}{2}f\theta' = 0. \tag{33}$$

Equation (32) is decoupled from the energy equation (33).

Case(3): For this case when $\phi = 0$; the physical parameters $n = 0$, $Nr = 0$, $Ec = 0$, $D_f = 0$, $Gr_t = 0$ and $Gr_c = 0$, (15)-(16) reduce to (see Yih [30]):

TABLE I
Thermophysical Properties of the Base Fluid and the Nanoparticles, (See [34], [25])

Physical properties	Base fliud (Water)	Copper (Cu)	Silver (Ag)
$C_p(J/kgK)$	4179	385	235
$\rho(Kg/m^3)$	997.1	8933	10500
$k(W/mK)$	0.613	401	429
$\alpha \times 10^7(m^2/s)$	1.47	1163.1	1738.6
$\beta \times 10^5(K^{-1})$	21	1.67	1.89

TABLE II
Comparison of the Values of $-f''(0,0)$ for Various Values of n, when $\phi = 0$(Regular Fluid), $Gr_t = Gr_c = 0$ and $\xi = 0$ (Steady State)

	Yih[30]	Present result (SRM)
n	$-f''(0,0)$	$-f''(0,0)$
-0.05	0.213484	0.213685
0.0	0.332057	0.332058
1/3	0.757448	0.757406

$$f''' + \frac{1}{2}ff'' + \xi(1 - f') =$$
$$\xi\left[f'\frac{\partial f'}{\partial \xi} - f''\frac{\partial f}{\partial \xi}\right] \tag{34}$$

$$\frac{1}{Pr}\theta'' + \frac{1}{2}f\theta' = \xi\left[f'\frac{\partial \theta}{\partial \xi} - \theta'\frac{\partial f}{\partial \xi}\right] \tag{35}$$

subject to the boundary conditions (18). Equations (15)-(17) were solved using the SRM, Motsa [29].

The SRM is an iterative procedure that employs the Gauss-Seidel type of relaxation approach to linearize and decouple the system of differential equations. Further details of the rules of the SRM can be found in ([35], [36]). The linear terms in each equation are evaluated at the current iteration level (denoted by $r+1$) and the non-linear terms are assumed to be known from the previous iteration level (denoted by r).

TABLE III
Comparison of the Values of $-\theta'(0,0)$ for Various Values of Pr, when $\phi = 0$, $Nr = Ec = D_f = n = 0$ and $\xi = 0$ (Steady State)

	Yih[30]	Present result (SRM)
Pr	-$\theta'(0,0)$	-$\theta'(0,0)$
0.1	0.140034	0.140034
1.0	0.332057	0.332057
10	0.728141	0.728141
100	1.571831	1.571658
1000	3.387083	3.396962
10000	7.297402	7.351156

TABLE IV
Comparison of the Values of $-\theta'(0,\xi)$ for Various Values of Pr and ξ with $\phi = 0$ (Regular Fluid), $Nr = Ec = D_f = n = 0$

		Yih[30]	Present results
Pr	ξ	-$\theta'(0,\xi)$	-$\theta'(0,\xi)$
	0.0	0.297526	0.297526
	0.5	0.357022	0.356986
0.733	1.0	0.382588	0.382558
	1.5	0.398264	0.398239
	2.0	0.409168	0.409147
	0.0	0.332057	0.332057
	0.5	0.402864	0.402822
1.0	1.0	0.433607	0.433572
	1.5	0.452634	0.452604
	2.0	0.465987	0.465962

The linearized form of (15) - (17) is

$$f'''_{r+1} + a_{1,r} f''_{r+1} + a_{2,r} f'_{r+1} - \phi_1 \xi (1-n) f'_{r+1} \frac{\partial f'_{r+1}}{\partial \xi} = R_{1,r}, \quad (36)$$

$$\theta''_{r+1} + b_{1,r} \theta'_{r+1} + b_{2,r} \theta_{r+1} - \frac{k_f}{k_{nf}} Pr \phi_2 \xi (1-n) f'_{r+1} \frac{\partial \theta_{r+1}}{\partial \xi} = R_{2,r}, \quad (37)$$

$$\phi''_{r+1} + c_{r,1} \phi'_{r+1} + c_{2,r} \phi_{r+1} - Sc \xi (1-n) f'_{r+1} \frac{\partial \phi_{r+1}}{\partial \xi} = R_{3,r}, \quad (38)$$

where

$$a_{1,r} = \phi_1 \left[\frac{(n+1)}{2} f_r + (1-n) \xi \frac{\partial f'_r}{\partial \xi} \right], \quad a_2 = -\phi_1 \xi,$$
$$R_{1,r} = -\phi_1 [\xi (1 - f'^2_r) + \xi + Gr_t \theta_r + Gr_c \phi_r],$$
$$b_{1,r} = \frac{k_f}{k_{nf}} Pr \phi_2 \left[\frac{(n+1)}{2} f_{r+1} + \xi (1-n) \frac{\partial f_{r+1}}{\partial \xi} \right],$$
$$b_{2,r} = -\frac{k_f}{k_{nf}} Pr \phi_2 \xi f'_{r+1},$$
$$R_{2,r} = -\frac{k_f}{k_{nf}} Pr D_f \Phi_r - \frac{k_f}{k_{nf}} Pr \frac{Ec}{(1-\phi)^{2.5}} (f''_{r+1})^2,$$
$$c_{1,r} = \frac{(n+1)}{2} f_{r+1} Sc + Sc \xi (1-n) \frac{\partial f_{r+1}}{\partial \xi},$$
$$c_{2,r} = -Sc[2n f'_{r+1} + \gamma],$$
$$R_{3,r} = -ScSr \theta''_{r+1}.$$

It must be noted that (36)-(38) are linear and being decoupled, can be solved sequentially to obtain approximate solutions $f(\eta, \xi)$, $\theta(\eta, \xi)$ and $\phi(\eta, \xi)$. In this study, the Chebyshev spectral collocation method was used to discretize in η and finite differences with central differencing for is used to discretize in ξ. Starting from initial guesses for f, θ and ϕ, (36)-(38) were solved iteratively until the approximate solutions converged to within a certain prescribed tolerance level. The accuracy of the results was validated against results from literature for some special cases of the governing equations.

V. Results and Discussion

In this study, we considered the flow of two nanofluids, namely Cu-water and Ag-water nanofluids. The conservation equations are solved numerically using the spectral relaxation method for $0 \leq \xi \leq 1$.

The thermophysical properties of the nanofluids and the base fluid water used in the numerical simulations are given in Table I. To determine the accuracy of our numerical results, we have compared our results for the local skin friction coefficient and the local Nusselt number with previous results by Yih [30]. The results are shown in Tables II-IV. The comparison with previously published results shows excellent agreement which is useful in establishing the validity of our approach. The Nusselt number for various values of the Prandtl number Pr and ξ are given in Tables III and IV.

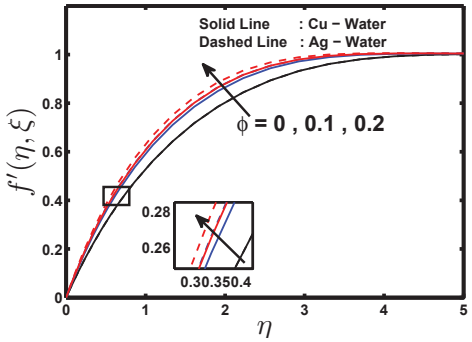

Fig. 3 Effect of change in the nanoparticle volume fraction values ϕ on velocity profiles for $Gr_t = 0.01$, $n = 0$, $Gr_c = 0.01$, $Nr = 10$, $Pr = 7$,$Ec = 10$, $D_f = 0.01$, $\gamma = 3$, $Sc = 1$, $Sr = 1$ and $\xi = 0.5$

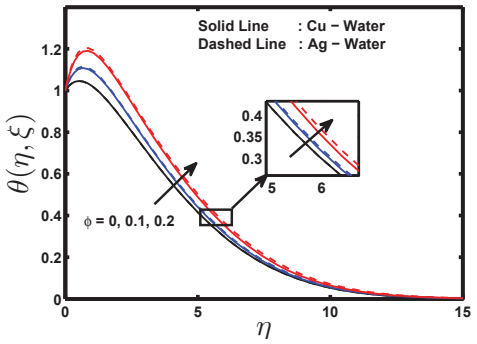

Fig. 4 Effect of change in the nanoparticle volume fraction values ϕ on temperature profiles for $Gr_t = 0.01$, $n = 0$, $Gr_c = 0.01$, $Nr = 10$, $Pr = 7$,$Ec = 10$, $D_f = 0.01$, $\gamma = 3$, $Sc = 1$, $Sr = 1$ and $\xi = 0.5$

Figs. 2-8 show the effect of nanoparticle volume fraction on the velocity profiles, temperature profiles, concentration profiles, skin friction coefficient, heat transfer coefficient and the mass transfer coefficient respectively. Increased nanoparticle volume fraction leads to an increase in the fluid velocity, temperature profiles and the mass transfer coefficient while the concentration profiles, skin friction coefficient and heat transfer coefficients are reduced. Figs. 6 and 7 show that the skin friction and the heat transfer coefficient decrease with the increasing value of ξ, whereas in Figs. 8 the mass

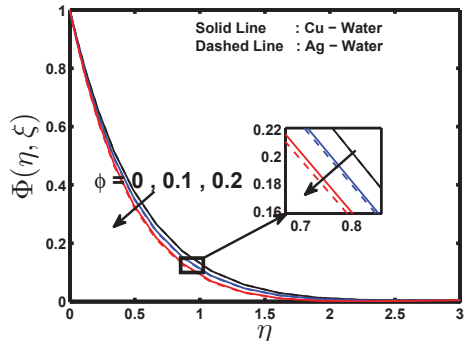

Fig. 5 Effect of change in the nanoparticle volume fraction values ϕ on concentration profiles for $Gr_t = 0.01$, $n = 0$, $Gr_c = 0.01$, $Nr = 10$, $Pr = 7$,$Ec = 10$, $D_f = 0.01$, $\gamma = 3$, $Sc = 1$, $Sr = 1$ and $\xi = 0.5$

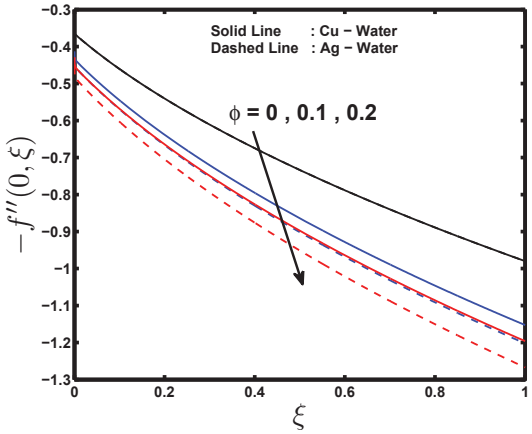

Fig. 6 Effect of change in the nanoparticle volume fraction values ϕ on Skin friction coefficient for $Gr_t = 0.01$, $n = 0$, $Gr_c = 0.01$, $Nr = 10$, $Pr = 7$,$Ec = 10$, $D_f = 0.01$, $\gamma = 3$,$Sc = 1$ and $Sr = 1$

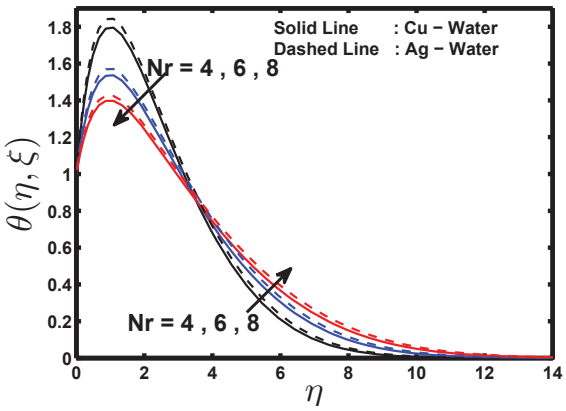

Fig. 9 Effect of thermal radiation Nr on temperature profiles for $n = 0$, $\phi = 0.3$, $Gr_t = 0.01$, $Gr_c = 0.01$, $Pr = 7$, $Ec = 10$, $D_f = 0.01$, $\gamma = 3$, $Sc = 1$, $Sr = 1$ and $\xi = 0.5$

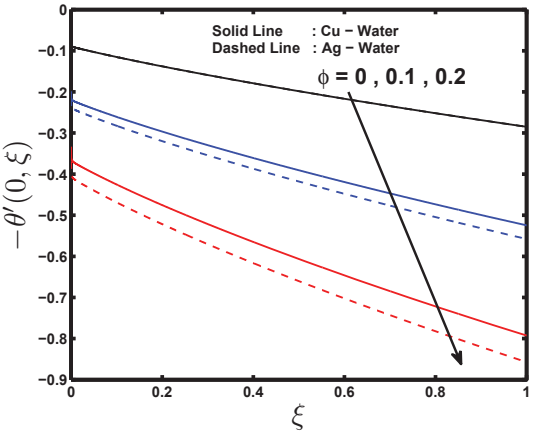

Fig. 7 Effect of change in the nanoparticle volume fraction values ϕ heat transfer coefficient for $Gr_t = 0.01$, $n = 0$, $Gr_c = 0.01$, $Nr = 10$, $Pr = 7$,$Ec = 10$, $D_f = 0.01$, $\gamma = 3$,$Sc = 1$ and $Sr = 1$

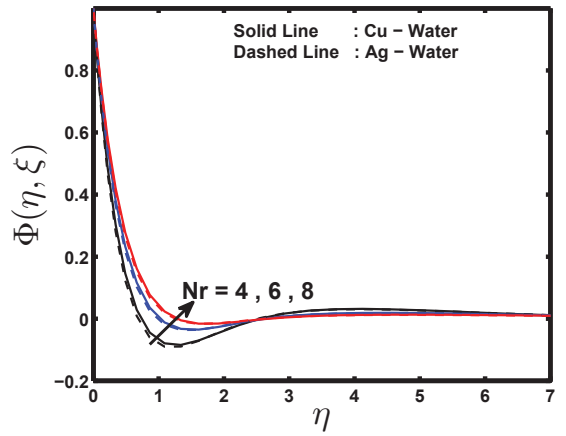

Fig. 10 Effect of thermal radiation Nr on concentration profiles for $n = 0$, $\phi = 0.3$, $Gr_t = 0.01$, $Gr_c = 0.01$, $Pr = 7$, $Ec = 10$, $D_f = 0.01$, $\gamma = 3$, $Sc = 1$, $Sr = 1$ and $\xi = 0.5$

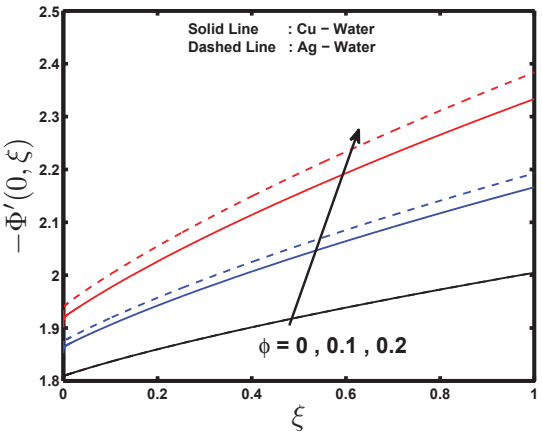

Fig. 8 Effect ofchange in the nanoparticle volume fraction values ϕ on mass transfer coefficient for $Gr_t = 0.01$, $n = 0$, $Gr_c = 0.01$, $Nr = 10$, $Pr = 7$,$Ec = 10$, $D_f = 0.01$, $\gamma = 3$,$Sc = 1$ and $Sr = 1$

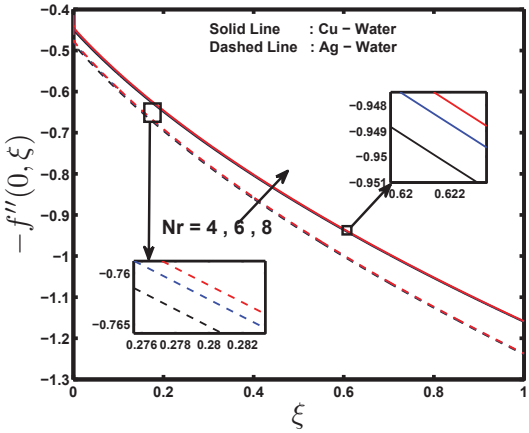

Fig. 11 Effect of thermal radiation Nr on Skin friction coefficient for $n = 0$, $\phi = 0.3$, $Gr_t = 0.01$, $Gr_c = 0.01$, $Pr = 7$, $Ec = 10$, $D_f = 0.01$, $\gamma = 3$, $Sc = 1$ and $Sr = 1$

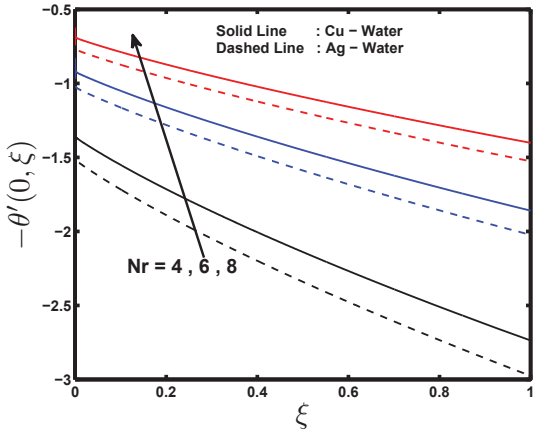

Fig. 12 Effect of thermal radiation Nr on heat transfer coefficient for $n = 0$, $\phi = 0.3$, $Gr_t = 0.01$, $Gr_c = 0.01$, $Pr = 7$, $Ec = 10$, $D_f = 0.01$, $\gamma = 3$, $Sc = 1$ and $Sr = 1$.

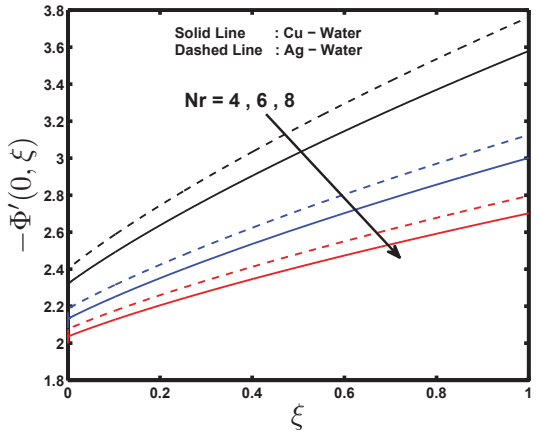

Fig. 13 Effect of thermal radiation Nr on mass transfer coefficient for $n = 0$, $\phi = 0.3$, $Gr_t = 0.01$, $Gr_c = 0.01$, $Pr = 7$, $Ec = 10$, $D_f = 0.01$, $\gamma = 3$, $Sc = 1$ and $Sr = 1$.

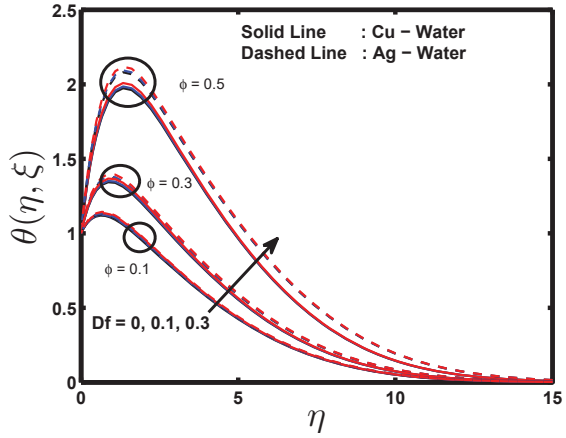

Fig. 14 Effect of the Dufour number on temperature profiles with nanofluid $\phi = 0.1, 0.3, 0.5$ for $n = 0$, $Gr_t = 0.05$, $Gr_c = 0.1$, $Pr = 7$, $Nr = 10$, $Ec = 9$, $\gamma = 0.3$, $Sc = 2$, $Sr = 1$ and $\xi = 0.5$.

transfer coefficient increases with the increasing value of. This is due to the fact that increased nanoparticle volume

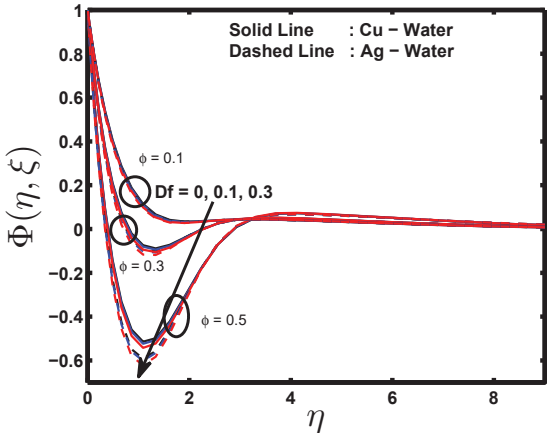

Fig. 15 Effect of the Dufour number on concentration profiles with nanofluid $\phi = 0.1, 0.3, 0.5$ for $n = 0$, $Gr_t = 0.05$, $Gr_c = 0.1$, $Pr = 7$, $Nr = 10$, $Ec = 9$, $\gamma = 0.3$, $Sc = 2$, $Sr = 1$ and $\xi = 0.5$.

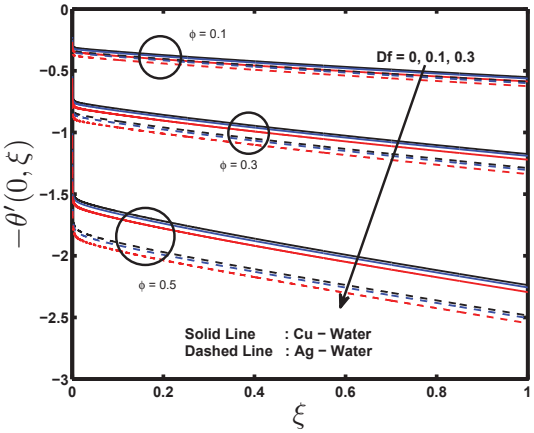

Fig. 16 Effect of the Dufour number on heat transfer coefficient with nanofluid $\phi = 0.1, 0.3, 0.5$ for $n = 0$, $Gr_t = 0.05$, $Gr_c = 0.1$, $Pr = 7$, $Nr = 10$, $Ec = 9$, $\gamma = 0.3$, $Sc = 2$ and $Sr = 1$.

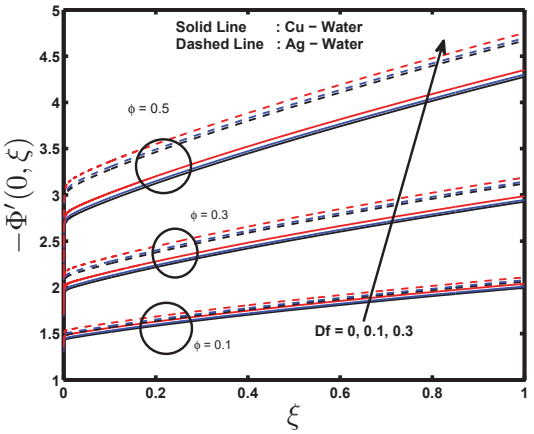

Fig. 17 Effect of the Dufour number on mass transfer coefficient with nanofluid $\phi = 0.1, 0.3, 0.5$ for $n = 0$, $Gr_t = 0.05$, $Gr_c = 0.1$, $Pr = 7$, $Nr = 10$, $Ec = 9$, $\gamma = 0.3$, $Sc = 2$ and $Sr = 1$.

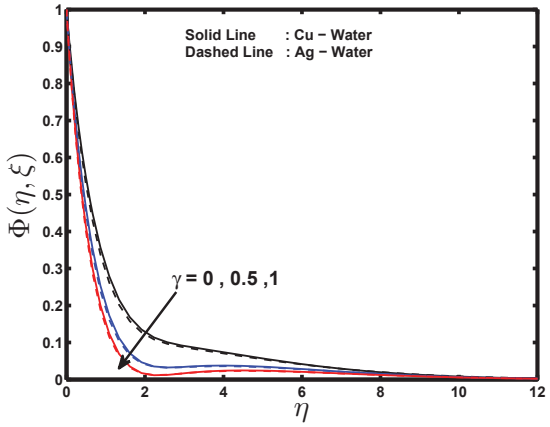

Fig. 18 Effect of chemical reaction parameter γ on concentration profiles for $n = 0$, $\phi = 0.3$, $Gr_t = 0.01$, $Gr_c = 0.01$, $Pr = 7$, $Nr = 10$, $Ec = 10$, $D_f = 0.01$, $Sc = 1$, $Sr = 1$ and $\xi = 0.5$.

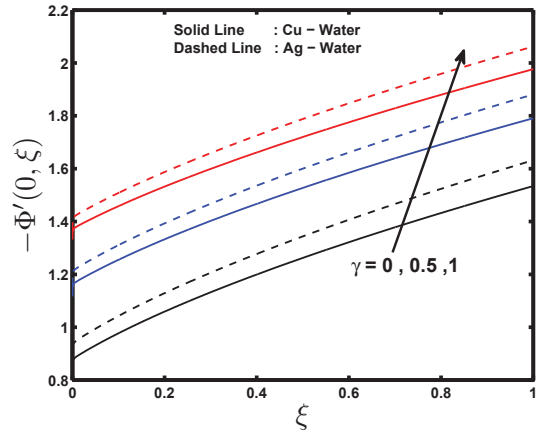

Fig. 19 Effect of chemical reaction parameter γ on the local Sherwood number for $n = 0$, $\phi = 0.3$, $Gr_t = 0.01$, $Gr_c = 0.01$, $Pr = 7$, $Nr = 10$, $Ec = 10$, $D_f = 0.01$, $Sc = 1$ and $Sr = 1$.

fraction enhances the thermal conductivity causing higher flow rates at the surface. Comparing the effect of the nanoparticle volume fraction on Cu-water and Ag-water nanofluids, (Figs. 2-4 and 8) it is noted that the effect is greater in the case of a Ag-water nanofluid than in a Cu-water nanofluid. The reverse is true for solutal concentration profiles, skin friction coefficient and the heat transfer coefficient where the effect is greater for Cu-water nanofluids (see Figs. 5-7). These finding are similar to the results reported by Kameswaran et al. [37]. Figs. 9-13 show the influence of the thermal radiation parameter on the temperature profiles, concentration profiles, skin friction coefficient, heat transfer coefficient and mass transfer coefficient. Fig. 9 indicates that as η increase, the temperature profile increases correspondingly up to a certain range and after that it shows the opposite trend. The results show a greater sensitivity for a Ag-water nanofluid regarding the temperature profiles, and mass transfer coefficient while the Cu-water nanofluid is more sensitive for concentration profile, the skin friction coefficient and the heat transfer coefficient. These results are qualitatively similar to those obtained by Kameswaran and Sibanda [38].

Figs. 14-17 show the effects of the Dufour number for different values of the nanoparticle volume fraction ($\phi = 0.3$, $0.5, 0.7$) on the temperature profiles, concentration profiles, heat transfer coefficient and mass transfer coefficient, respectively. The temperature profiles and mass transfer coefficient increase with increases in the Dufour number while the concentration profiles and heat transfer coefficient are reduced with increasing value of Dufour number. As with the previous set of graphs, the Ag-water nanofluid shows a greater sensitivity to increases in the Dufour number compared to the Cu-water nanofluid. The heat transfer coefficient is greater for a Cu-water nanofluid.

Figs. 18 and 19 show the effect of the chemical reaction parameter on the concentration profiles and the mass transfer coefficient. The local solute concentration is reduced by the increasing reaction rate. The concentration profiles decrease with an increase in the chemical reaction parameter whereas the mass transfer coefficient increases with an increase in the chemical reaction parameter. The mass transfer coefficient increases as ξ increases.

Figs. 20 and 21 show the impact of the Soret number on the concentration profiles and the mass transfer coefficient. Where the concentration profiles grow less while the mass transfer coefficient increases with an increase in the Soret number. Again Figs. 20 and 21 show that as Soret number increases, the boundary layer thickness for the solute concentration reduces. The mass transfer coefficient is increasing when the Soret number is positive.

VI. Conclusion

The steady state mixed convection in MHD nanofluid boundary layer flow and heat, mass transfer from a non-isothermal wedge has been studied. We have considered the flow of Cu-water and Ag-water nanofluids and assumed that the nanoparticle volume fraction can be actively controlled at the boundary surface. The equations were solved using the spectral relaxation method and to benchmark our solutions, these were compared with some limiting cases in the literature. The comparison showed a good agreement with the published results. From the numerical simulations, the following conclusions may drawn;

1) The velocity profiles increase with increases in the nanoparticle volume fraction.
2) The temperature profiles increase with increasing nanoparticle volume fraction, thermal radiation parameter and the Dufour number.
3) The concentration profiles decrease with increasing nanoparticle volume fraction, chemical reaction parameter, Soret and Dufour numbers while the concentration profiles increase with increases in the thermal radiation parameter.
4) The skin friction coefficient decreases with an increase in the nanoparticle volume fraction while the opposite trend is observed for increasing thermal radiation parameter values.

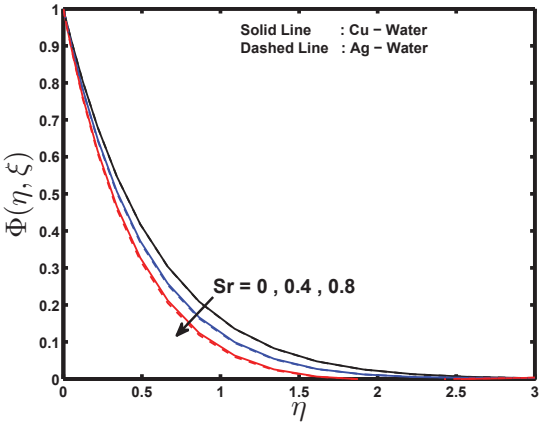

Fig. 20 Effect of the Soret number on the concentration profiles for $n = 0$, $\phi = 0.3$, $Gr_t = 0.01$, $Gr_c = 0.01$, $Pr = 7$, $Nr = 10$, $Ec = 10$, $D_f = 0.01$, $Sc = 1$ and $\gamma = 3$.

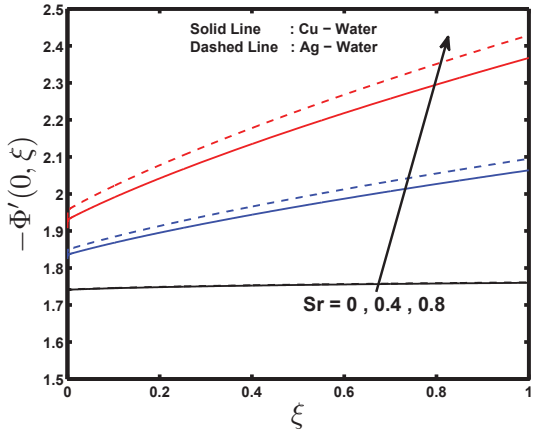

Fig. 21 Effect of the Soret number on the local Sherwood number for $n = 0$, $\phi = 0.3$, $Gr_t = 0.01$, $Gr_c = 0.01$, $Pr = 7$, $Nr = 10$, $Ec = 10$, $D_f = 0.01$, $Sc = 1$ and $\gamma = 3$.

5) The heat transfer coefficient decreases with an increase in the nanoparticle volume fraction and the Dufour number while the heat transfer coefficient increase with an increase in the values of thermal radiation parameter.
6) The mass transfer coefficient increases with an increase in the nanoparticle volume fraction, chemical reaction parameter, Soret and Dufour number while the opposite trend is observed for increasing values of thermal radiation parameter.

Acknowledgment

The authors would like to thank the University of KwaZulu-Natal and Claude Leon Foundation, South Africa for the financial support.

References

[1] A. Subhas, P. H. Veena, "Visco-elastic fluid flow and heat transfer in porous medium over a stretching sheet", *Int. J. Non-linear Mech.* vol. 33, pp, 531–540, 1998.
[2] K. V. Prasad, M. S. Abel, A. Joshi, "Oscillatory motion of a visco-elastic liquid over a stretching sheet in porous media", *J. Porous Media*, vol. 3, PP. 61–68, 2000.
[3] H. Blasius, "Grenzschichten in Flussigkeiten Mit Kleiner Reibung", *Zeitschrift für Angewandte Mathematik und Physik*, vol. 56, pp. 1–37, 1908.
[4] L. Howarth, "On the solution of the laminar boundary layer equations", *Proceedings of the Society of London, Mathematical and Physical Sciences*, vol. 919, pp. 547–579, 1938.
[5] L. J. Crane, "Flow past a stretching plate", *Zeitschrift für Angewandte Mathematik und Physik, ZAMP* vol. 21, pp. 645–647, 1970.
[6] P. S. Gupta, A. S. Gupta, "Heat and mass transfer on a stretching sheet with suction or blowing", *Can. J. Chem. Eng.*, vol. 55, pp. 744–746, 1977.
[7] Y. M. Aiyesimi, S. O. Abah, G. T. Okedayo, "The analysis of hydromagnetic free convection heat and mass transfer flow over a stretching vertical plate with suction", *Amer. J. Comput. Appl. Math.*, vol. 1, pp. 20–26, 2011.
[8] S. J. Liao, "Series solutions of unsteady boundary layer flows over a stretching flat plate", *Studies Applied Mathematics*, vol. 117, pp. 239–263, 2006.
[9] H. Xu, S. J. Liao, I. Pop, "Series solutions of unsteady three-dimensional MHD flow and heat transfer in the boundary layer over an impulsively stretching plate", *Eur. J. Mech. B/Fluids*, vol. 26, pp. 15–27, 2007.
[10] H. Masuda, A. Ebata, K. Teramae, N. Hishinuma, "Alteration of thermal conductivity and viscosity of liquid by dispersing ultra-fine particles (dispersion of $-Al_2O_3, SiO_2$ and TiO_2 ultra-fine particles)", *Netsu. Bussei.*, vol. 7, pp. 227–233, 1993.
[11] J. Buongiorno, W. Hu, "Nanofluid coolants for advanced nuclear power plants", *Proceedings of ICAPP05*, Seoul, 15-19 May 2005, vol. 5, pp. 15–15.
[12] S. Choi, Z. Zhang, W. Yu, F. Lockwood, E. Grulke, "Anomalously thermal conductivity enhancement in nanotube suspensions", *Appl. Phys. Letters*, vol. 79, pp. 2252–2254, 2001.
[13] N. A. H. Haroun, S. Mondal, P. Sibanda, S. S. Motsa, M. M. Rashidi, "Heat and mass transfer of nanouid through an impulsively vertical stretching surface using the spectral relaxation method", *Boundary Value Problems* vol. 2015, no. 161, pp. 1-16, 2015.
[14] N. A. H. Haroun, S. Mondal, P. Sibanda,"The effects of thermal radiation on an unsteady MHD axisymmetric stagnation- point flow over a shrinking sheet in presence of temperature dependent thermal conductivity with Navier slip", *PLoS One*, vol. 10, no. 9: e0138355. doi:10.1371/journal.pone.0138355, 2015.
[15] N. A. H. Haroun, S. Mondal, P. Sibanda, "Unsteady natural convective boundary-layer flow of MHD nanofluid over a stretching surfaces with chemical reaction using the spectral relaxation method: A revised model", *Procedia Engineering*, vol. 127, pp. 18 - 24, 2015.
[16] I. S. Oyelakin, S. Mondal, P. Sibanda, "Unsteady Casson nanofluid flow over a stretching sheet with thermal radiation, convective and slip boundary conditions", *Alexandria Engineering Journal*, vol. 55, no. 2, pp. 10251035, 2016.
[17] T. M. Agbaje, S. Mondal, Z. G. Makukula, S. S. Motsa, P. Sibanda, "A new numerical approach to MHD stagnation point flow and heat transfer towards a stretching Sheet",*Ain Shams Engineering Journal* doi:10.1016/j.asej.2015.10.015, 2016.
[18] J. A. Gbadeyan, A. S. Idowu, A. W. Ogunsola, O. O. Agboola, P. O. Olanrewaju, "Heat and mass transfer for Soret and Dufour's effect on mixed convection boundary layer flow over a stretching vertical surface in a porous medium filled with a viscoelastic fluid in the presence of magnetic field", *Global J. Sci. Front. Res.*, vol. 11, pp. 1–19, 2011.
[19] M. J. Subhakar, K. Gangadhar, "Soret and Dufour effects on MHD free convection heat and mass transfer flow over a stretching vertical plate with suction and heat source/sink", *Int. J. Modern Eng. Res.*, vol. 2, pp. 3458–3468, 2012.
[20] T. R. Mahapatra, S. Mondal, D. Pal, "Heat transfer due to magnetohydrodynamic stagnation-point flow of a power-law fluid towards a stretching surface in the presence of thermal radiation and suction/injection", *ISRN Thermodynamics* vol. 9, pp. 1–9, 2012.
[21] Md. S. Khan, Md. M. Alam, M. Ferdows, "Effects of magnetic field on radiative flow of a nanofluid past a stretching sheet", *Procedia Engineering* vol. 56, pp. 316–322, 2013.
[22] P. Singh, D. Sinha, N. S. Tomer, "Oblique stagnation-point Darcy flow towards a stretching sheet", *J. Appl. Fluid Mech.*, vol. 5, pp. 29–37, 2012.
[23] A. M. Rohni, S. Ahmad, Md. I. A. Ismail, I. Pop, "Flow and heat transfer over an unsteady shrinking sheet with suction in a nanofluid using Buongiorno's model", *Int. Commu. Heat Mass Trans.*, vol. 43, pp. 75–80, 2013.
[24] J. Buongiorno, "Convective transport in nanofluids", *ASME Journal of Heat Transfer*, vol. 128, pp. 240–250, 2006.

[25] H. F. Oztop, E. Abu-Nada, "Numerical study of natural convection in partially heated rectangular enclosures filled with nanofluids", *Int. J. Heat Fluid Flow*, vol 29 pp. 1326–1336, 2008.
[26] P.E. Gharagozloo,J. K. Eaton, K. E. Goodson, "Diffusion, aggregation, and the thermal conductivity of nanofluids",*Appl. Phys. Lett.* vol. 93, pp. 103110, http://dx.doi.org/10.1063/1.2977868, 2008.
[27] J. Philip, P. D. Shima, B. Raj, "Nanofluid with tunable thermal properties", *Appl. Phys. Lett.*, vol. 92, pp. 043108, http://dx.doi.org/10.1063/1.2838304, 2008.
[28] N. A. H. Haroun, P. Sibanda, S. Mondal, S. S. Motsa, "On unsteady MHD mixed convection in a nanofluid due to a stretching/shrinking surface with suction/injection using the spectral relaxation method", *Boundary Value Problems*, vol. 15, pp. 1–17, 2015.
[29] S. S. Motsa, "A new spectral relaxation method for similarity variable nonlinear boundary layer flow systems", *Chem. Eng. Commu.*, vol. 16, pp. 23–57, 2013.
[30] K. A. Yih, "MHD forced convection flow adjacennt to a non-isothermal wedge", *Int. Commun. Heat Mass Trans.*, vol. 26, pp. 819–827, 1999.
[31] R. K. Tiwari, M. K. Das, "Heat transfer augmentation in a two-sided lid-driven differentially heated square cavity utilizing nanofluids", *Int. J. Heat Mass Trans.*, vol. 50, pp. 2002–2018, 2007.
[32] H. C. Brinkman, "The viscosity of concentrated suspensions and solution", *J. Chem. Phys.* vol. 20, pp. 571–581, 1952.
[33] E. Abu-Nada, "Application of nanofluids for heat transfer enhancement of separated flows encountered in a backward facing step", *Int. J. Heat Fluid Flow*, vol. 29, pp. 242–249, 2008.
[34] M. Sheikholeslami, M. G. Bandpy, D. D. Ganji, S. Soleimani, S. M. Seyyedi, "Natural convection of nanofluids in an enclosure between a circular and a sinusoidal cylinder in the presence of magnetic field", *Int. Commun. Heat Mass Trans.*, vol. 39, pp. 1435–1443, 2012.
[35] S. S. Motsa, P. G. Dlamini, M. Khumalo, "Spectral relaxation method and spectral quasilinearization method for solving unsteady boundary layer flow problems", *Adv. Math. Phys.*, vol. 12, Article ID 341964, doi 10.1155/2014/341964, 2014.
[36] S. S. Motsa, Z. G. Makukula, "On spectral relaxation method approach for steady von Karman flow of a Reiner-Rivlin fluid with Joule heating and viscous dissipation", *Cent. Eur. J. Phys.*, vol. 11, pp. 363–374, 2013.
[37] P. K. Kameswaran, M. Narayana, P. Sibanda, P. V. S. N. Murthy, "Hydromagnetic nanofluid flow due to a stretching or shrinking sheet with viscous dissipation and chemical reaction effects", *Int. J. Heat Mass Trans.*, vol. 55, pp. 7587–7595, 2012.
[38] P. K. Kameswaran, P. Sibanda, "Thermal dispersion effects on convective heat and mass transfer in an Ostwald de Waele nanofluid flow in porous media", *Boundary Value Problems*, vol. 10, pp. 1–12, 2013.

Nageeb A.H. Haroun is a Ph.D. student in School of Mathematics, Statistics and Computer Science at University of KwaZulu-Natal, Pietermaritzburg, Private Bag X01, Scottsville-3209,South Africa. His Ph.D. topic is "Convective heat and mass transfer in boundary layer flow through porous a medium saturated with nanofluids". He has completed his M.Sc. from the same university. His research interest is computational fluid dynamics.

Sabyasachi Mondal is Post Doctoral Research Fellow in School of Mathematics, Statistics and Computer Science at University of KwaZulu-Natal, Pietermaritzburg, Private Bag X01, Scottsville-3209,South Africa since 2014. He has completed his Ph.D. from Visva-Bharati university, Santiniketan, West Bengal, India in 2013. His research interests are in nanofluid flow, heat and mass transfer in cavity and boundary layer flows etc.

Precious Sibanda is a Professor in in School of Mathematics, Statistics and Computer Science at University of KwaZulu-Natal, Pietermaritzburg, Private Bag X01, Scottsville-3209,South Africa. His research interests are in heat and mass transfer problems, nanofluid flow, bio-mathematics, hydrodynamic stability and mathematical modelling etc. in general.